LANGMUIR

pubs.acs.org/Langmuir Article

Mitigating Membrane Biofouling in Protein Production with Zwitterionic Peptides

Published as part of Langmuir special issue "2025 Pioneers in Applied and Fundamental Interfacial Chemistry: Shaoyi Jiang".

Boran Sun, Junneng Wen, Meng Qin, Pranay Ladiwala, David Stern, Ziying Xu, Michael J. Betenbaugh, and Honggang Cui*

Cite This: *Langmuir* 2025, 41, 1057−1067 Read Online

ACCESS | Metrics & More | Article Recommendations | Supporting Information

ABSTRACT: Biofouling on polymeric membranes poses a significant challenge in protein production and separation processes. We report here on the use of zwitterionic peptides composed of alternating lysine (K) and glutamic acid (E) residues to reduce biomolecular fouling on gold substrates and polymeric membranes within a protein production-mimicking environment. Our findings demonstrate that both gold chips and polymeric membranes functionalized with longer sequence zwitterionic peptides, along with a hydrophilic linker, exhibit superior antifouling performance across various protein-rich environments. Furthermore, increasing the grafting density of these peptides on substrates enhances their antifouling properties. We believe that this work sheds light on the antifouling capabilities of zwitterionic peptides in cell culture environments, advancing our understanding and paving the way for the development of zwitterionic peptide-based antifouling materials for polymeric membranes.

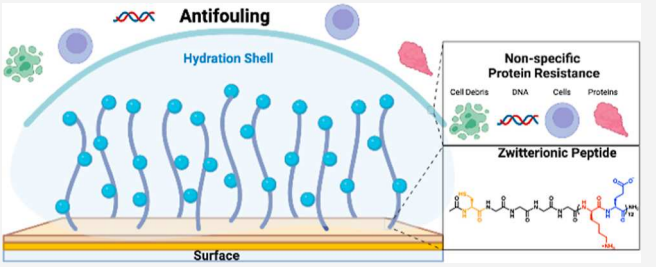

INTRODUCTION

The gradual buildup of proteins, cellular debris, and other substances on substrate surfaces over time, particularly under biological and physiological conditions,[1,2] poses significant challenges in various fields such as drug delivery, water treatment, protein separation, among others.[3−8] Efforts to address fouling-related issues and to devise effective solutions have been a central focus of extensive research over the past few decades.[8−13] One commonly employed strategy for preventing surface fouling is the chemical modification of surfaces with poly(ethylene glycol) (PEG)[14,15] or zwitterionic polymers.[16−18] These methods are intended to minimize the accumulation of biomolecules, inhibit microbial adhesion, and curb biofilm formation on various surfaces, particularly in medical devices and related applications.[19−22] While PEG and its shorter variant, oligo(ethylene glycol) (OEG), are commonly used as coatings to resist foulant adsorption,[23] their susceptibility to oxidation and degradation over time and conformational instability in high ionic strength buffers presents a considerable obstacle.[15] In this context, zwitterionic polymeric materials, known for their robust antifouling properties and stability in high-salt conditions, have emerged as promising alternatives.[24−28]

Zwitterionic polymers are characterized by an equal number of closely positioned negatively charged and positively charged groups within their structure.[13] These polymers promote surface hydration through ionic solvation, creating a dense hydration shell that establishes a high-energy barrier against fouling.[28−31] Early research by the Jiang Lab pioneered the investigation of antifouling properties in zwitterionic polymers,[5,8,13] particularly with phosphorylcholine (PC)-based systems,[32,33] which exhibited superior resistance to protein adsorption and cellular adhesion while maintaining charge neutrality. Building upon this foundational work, subsequent advancements in carboxybetaine (CB)-based[34−38] and sulfobetaine (SB)-based[31,38−41] zwitterionic polymers have demonstrated their ultralow fouling capabilities, establishing a new paradigm in surface modification strategies. Despite the extensive body of research on zwitterionic polymers, investigations into the antifouling properties of zwitterionic peptides remain relatively limited, particularly under cell culture and various protein production conditions. Zwitterionic peptides, comprising an equal number of positively and negatively charged amino acid residues, offer enhanced design versatility and biocompatibility compared to polybetaines.[42−44]

Received: November 1, 2024
Revised: December 12, 2024
Accepted: December 18, 2024
Published: January 6, 2025

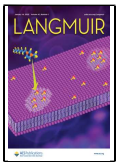

https://doi.org/10.1021/acs.langmuir.4c04384
Langmuir 2025, 41, 1057−1067

While previous studies have demonstrated the antifouling properties of zwitterionic peptide coatings and some important molecular design criteria,[6,45−49] comprehensive evaluations under diverse conditions, such as a protein production environment and extreme lysed cell environments, remain largely unexplored.

In this study, we selected zwitterionic peptides for their versatile design possibilities offered by peptide motifs and their superior biocompatibility under cell culture conditions.[50,51] By attaching these peptides to a gold substrate, we demonstrated their antifouling properties against various testing solutions, including protein solutions, cell culture media, and lysed cell solutions. Furthermore, we developed a new membrane modification strategy by functionalizing zwitterionic peptides onto a poly(ether sulfone) (PES) membrane and verified the antifouling performance of the modified membranes under different conditions. These rationally designed peptides exhibited strong resistance to foulants even under extreme lysed cell conditions, highlighting the excellent antifouling capabilities of zwitterionic peptides.

MATERIALS AND METHODS

Chemicals and Materials. All Fmoc amino acids including Rink-Amide and *O*-benzotriazole-*N*,*N*,*N*′,*N*′-tetramethyluronium-hexafluoro-phosphate (HBTU) were purchased from Advanced Automated peptide Protein Technologies (AAPTEC, Louisville, KY, USA). Silicon wafer chips with 100 nm gold were purchased from Platypus Technologies (Madison, WI, USA). PES was kindly provided by MilliporeSigma (Burlington, MA, USA). Pure human immunoglobulin G1 (IgG1) was obtained from Bristol Myers Squibb (Boston, MA, USA). *N*-(3,4-Dihydroxyphenethyl)methacrylamide (dopamine methacrylamide) was purchased from Polymer Source Inc. (Dorval, Montreal, Canada). The LIVE/DEAD Viability/Cytotoxicity Kit was purchased from Fisher Scientific (Suwanee, GA, USA). The HEK 293 cell line was purchased from American Type Culture Collection (ATCC, Manassas, VA). Dulbecco's modified Eagle's medium (DMEM)/high glucose, trypsin−EDTA (0.25%), phenol red, and PBS were obtained from Thermo Fisher Scientific (Carlsbad, CA, USA). Other reagents were sourced from Sigma-Aldrich (St Louis, MO, USA) or VWR (Randor, PA, USA) unless otherwise specified.

Synthesis and Purification of Zwitterionic Peptides. All the peptides were synthesized using the standard 9-fluorenylmethoxycarbonyl (Fmoc) solid-phase synthesis technique and D-amino acids. The peptide KE_8 was synthesized by the sequential conjugation of eight pairs of alternating Fmoc−D−Glu(OtBu)−OH amino acids and Fmoc−D−Lys(Boc)−OH amino acids, four Fmoc−Gly−OH amino acids, and one Fmoc−D−Cys(Trt)−OH on the Rink-Amide resin. 20% of 4-methylpiperidine in dimethylformamide (DMF) solution was used to deprotect the Fmoc. The amino acids were coupled onto the resin after the deprotection using a mixture of amino acids, HBTU and *N*,*N*-diisopropylethylamine (DIEA) (4:4:6 molar equivalence to free amine) in DMF for 2 h. Each conjugation of amino acids was followed by two rounds of Fmoc deprotection to ensure the availability of a free amine group on the amino acids. In the end, the cleavage of the resin was performed using a mixture of trifluoroacetic acid (TFA), triisopropylsilane (TIS), and water at a ratio of 92.5/5/2.5% v/v for 3 h. The solution containing the peptide and TFA was collected and concentrated in cold diethyl ether. The precipitate was washed with cold diethyl ether three times and centrifuged at 5000 rpm for 5 min. The crude peptide was dried under the hood overnight and allowed to stand for further purification. For purification, the crude peptide solid was dissolved in a water and acetonitrile (ACN) mixture containing 0.1% v/v NH_4OH and then purified by a Varian ProStar Model325 (Agilent Technologies, Santa Clara, CA) reverse-phase high-performance liquid chromatography (RP-HPLC) using a mobile phase of water and ACN. The peptide was separated from impurities by preparative RP-HPLC using a C_{18} column with a flow rate of 16 mL/min, 10 mL injections, and monitoring at 220 nm for peptide. The eluent gradient was run linearly from 10% to 40% ACN over 20 min. The collected fractions were analyzed by electrospray ionization mass spectrometry (ESI-MS) to isolate fractions containing the molecules of interest. Factions with the correct mass were combined, and excess ACN was removed using rotary evaporation. The peptides were lyophilized using a Labconco FreeZone freeze-dryer.

Gold Chip Pre-treatment and Modification. Gold-coated silicon wafers were obtained from Platypus Technologies (Madison, WI, USA). The gold chips were first immersed in Nanopure water and cleaned using a sonicator. They were then treated with a basic piranha solution (NH_4OH/H_2O_2, 7:3) at 75 °C for 20 min, followed by extensive rinsing with Nanopure water and drying with nitrogen gas. To remove any remaining moisture, the chips were stored in a vacuum desiccator. Subsequently, the gold chips underwent plasma cleaning (Denton evaporator) for 30 min to eliminate residual organic particles and enhance surface hydrophilicity by transferring electrons to the surface. Before use, the chips were rinsed with ethanol and Nanopure water three times and dried with nitrogen gas. Both the piranha solution and plasma cleaning were employed to remove organic matter and impurities while also increasing surface hydrophilicity. For peptide modification, the gold chips were incubated in a 1 mg/mL zwitterionic peptide solution prepared in PBS buffer for 24 h, resulting in zwitterionic peptide-modified gold chips.

Nonspecific Protein Adsorption Assays. Zwitterionic peptide-modified gold chips were rinsed with Nanopure water before use. A 1 mg/mL IgG protein solution was prepared for the protein adsorption test. Three zwitterionic peptide-modified gold chips, one regular peptide-modified gold chip, and one plain gold chip were incubated in the IgG protein solution for 4 h. After incubation, the gold chips were removed and rinsed thoroughly with a PBS solution to remove loosely bound proteins. The rinsed gold chips were then immersed in 4 mL of fresh PBS solution and sonicated for 5 min to dislodge any adsorbed proteins. UV−vis spectroscopy was used to measure the absorbance of the resulting solutions across a wavelength range of 600−200 nm. The absorbance values were subsequently converted to the adsorbed protein mass. The same procedure was applied to test adsorption in cell culture media and lysed cell media.

PES Membrane Pre-treatment and Modification. The PES membrane, delivered with a lubricant coating, was first rinsed with water to remove the lubricant. Dopamine methacrylamide (DM) was dissolved in Tris buffer (pH 8.5, 50 mM) to prepare a 1 M solution. The PES flat membranes were initially immersed in ethanol to clean the surface and then transferred to the DM solution. The membranes were shaken for 2 h at room temperature and subsequently allowed to settle overnight to preserve the pore structure.

After DM modification, the membranes were rinsed three times with Nanopure water to remove excess DM and minimize nonspecific adsorption. The membranes were then immersed in a 1 mM zwitterionic peptide solution and incubated for 3 days at room temperature to complete the modification process.

Grafting Density Tests. The grafting density of zwitterionic peptides on the PES-DM membrane was analyzed by using HPLC. A calibration curve correlating the concentration of KE12 peptides with the area under the curve was created using serial dilutions from 1 mM to 1 μM. A 1 mM KE12 solution was used as the stock solution to attach the zwitterionic peptides to the PES-DM membrane. Membranes were incubated in the stock solution for 1, 3, and 5 days to compare the effects of the incubation time. After incubation, the membranes were rinsed with Nanopure water to remove unattached peptides, and the rinsed solution was collected for analysis.

The concentration of KE12 in both the incubated and rinsed solutions was measured by HPLC to calculate the peptide grafting density. This was determined by subtracting the analyzed mass of unattached peptides from the total initial mass of KE12. The same procedure was applied to two additional conditions: varying the DM concentration and varying the KE12 concentration. For DM concentration tests, membranes were treated with 1, 3, and 5 mM

https://doi.org/10.1021/acs.langmuir.4c04384
Langmuir 2025, 41, 1057−1067

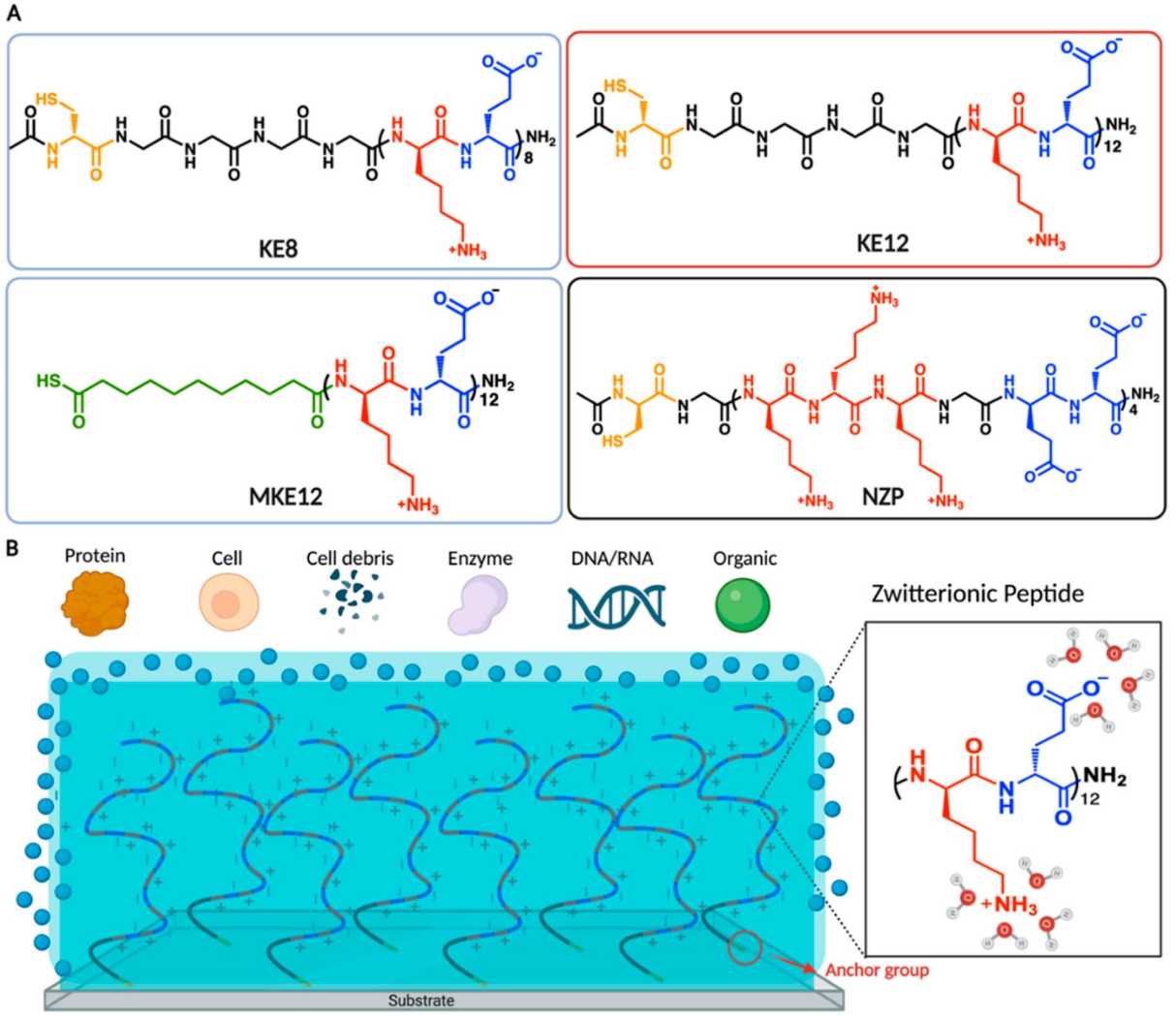

Figure 1. Molecular design and illustration of the zwitterionic peptide-modified substrate with antifouling properties. (A) Chemical structures of the four designed molecules. The three zwitterionic peptides (KE8, KE12, and MKE12) consist of varying numbers of lysine and glutamic acid pairs and feature different linker designs. NZP, the control peptide, lacks zwitterionic characteristics and consists of an unequal number of lysine and glutamic acid residues. (B) Schematic representation of the antifouling mechanism of zwitterionic peptide-modified substrates, depicting the formation of a hydration shell that repels foulants.

DM under three days of incubation with 1 mM KE12. For varying KE12 concentrations, membranes were incubated with 0.5, 1, and 1.5 mM KE12 while maintaining the DM concentration and incubation time constant.

Antifouling performance studies were conducted for each membrane using an IgG protein solution under different conditions, following the same procedure as that used for gold chip modification. The absorbance of IgG proteins was measured by UV−vis spectroscopy and converted into protein mass per unit area to quantify the antifouling performance.

Cell Viability Assays. The HEK 293 cell line was selected for the cell viability assay. Cells were passaged three generations before use and exposed to three concentrations of KE12 (0.4, 4, and 40 μM). Two control groups were included: a negative control (cells without peptide treatment) and a positive control (cells treated with ethanol). Approximately 10,000 cells per well were seeded on 8-well slides and cultured in DMEM for 12 or 24 h.

A 4 μM stock solution of ethidium homodimer-1 (EthD-1) was prepared in sterile DPBS, and 5 μL of the calcein AM stock solution was added to the EthD-1 solution. A total of 100 μL of the combined reagents was added to each well, followed by a 45 min incubation. Confocal microscopy was used to observe the fluorescence of the live and dead cells in each well. Calcein AM and EthD-1 exhibit excitation/emission wavelengths of 494/517 and 528/617 nm, respectively, allowing for the differentiation of live (green fluorescence) and dead (red fluorescence) cells.

Cell Culture and Peptide Cytotoxicity Tests. The CHOZN GS cell line cultured in proprietary media was used for spent media analysis. Fresh culture medium served as the Day 0 medium, while cell culture supernatant was collected on Day 5 of culture. Cell lysates were prepared by using the freeze−thaw method. Cell suspension samples were frozen at −80 °C for 30 min, followed by thawing at 37 °C for 30 min. This cycle was repeated three times to ensure complete cell lysis.

The CHOZN GS cell line (Sigma-Aldrich) was cultured in commercial medium (EX-Cell CD CHO Fusion) in both batch and fed-batch modes (Figure S7) for the viability study. Suspension cells were maintained in 125 mL shake flasks with a working volume of 30 mL and agitated at 125 rpm, at 37 °C, and under 5% carbon dioxide. Culture media supernatants were collected every 24 h to assess growth and viability, with Day 5 samples used for IgG titer measurements. Viable cell density was determined by using hemocytometry.

Protein A HPLC. Chromatographic measurements were performed by using an Agilent 1260 Infinity II LC System. A prepacked Protein A column (POROS A, 20 μm, 2.1 mm × 30 mm, 0.1 mL;

https://doi.org/10.1021/acs.langmuir.4c04384
Langmuir 2025, 41, 1057−1067

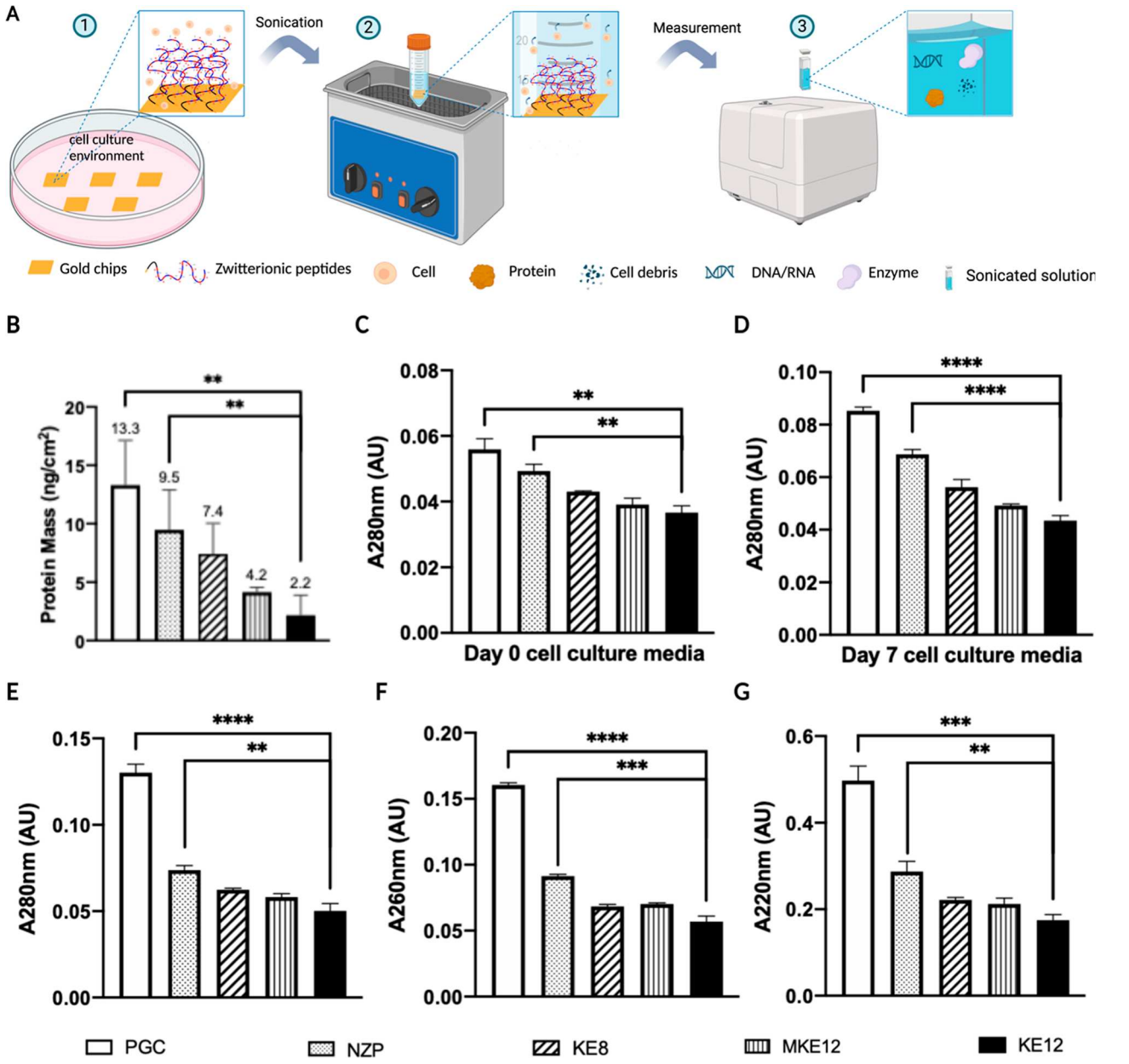

Figure 2. Evaluation of antifouling performance of zwitterionic peptide-modified gold chips. (A) Schematic of the antifouling performance assessment process, including cell environment incubation, surface sonication, and UV−vis measurement. (B) Quantification of IgG protein adsorption per unit area (cm^2) using UV−vis spectroscopy (the used IgG concentration was 1 mg/mL). (C) Adsorption of fresh cell culture media (Day 0) measured at 280 nm. (D) Adsorption of aged cell culture media (Day 7) measured at 280 nm. (E−G) Adsorption of lysed cell culture media at (E) 280 nm (proteins), (F) 260 nm (nucleic acids), and (G) 220 nm (amino acids). Each error bar represents the standard deviation of three independent measurements. Data are presented as mean ± SD (*p < 0.05; **p < 0.01; ns p > 0.05; ****p < 0.0001 for KE12 vs PGC and control NZP; unpaired t-test, n = 3).

Thermo Fisher Scientific, cat. no. 2100100) was employed for titer quantification. The binding buffer (Buffer A) consisted of 10 mM phosphate buffer with 100 mM sodium chloride at pH 7.2, while the elution buffer (Buffer B) consisted of 12 mM hydrochloric acid and 100 mM sodium chloride at pH 2.7. Absorbance was recorded at 280 nm. Harvested cell culture (HCC) samples were filtered through a 0.22 μm filter prior to HPLC analysis.

RESULTS AND DISCUSSION

Molecular Design and Substrate Modification. In designing the zwitterionic peptides, our goal was to achieve a zwitterionic characteristic by incorporating alternating positively and negatively charged natural amino acid residues. Figure 1A illustrates the molecular design of four different peptides, where we varied the number of charged groups and linker designs to identify key determinants of the antifouling performance. The first peptide, KE8, consists of 8 pairs of lysine (K) and glutamic acid (E) residues, where lysine provides the positive charge, and glutamic acid provides the negative charge. Four glycine (G) residues serve as a flexible linker for the zwitterionic peptides, followed by a cysteine anchor group. The cysteine residue, containing a thiol group, facilitates surface modification through well-defined thiol-gold chemistry or thiol−ene chemistry. The second peptide, KE12, shares a similar design with KE8 but incorporates 12 pairs of

https://doi.org/10.1021/acs.langmuir.4c04384
Langmuir 2025, 41, 1057−1067

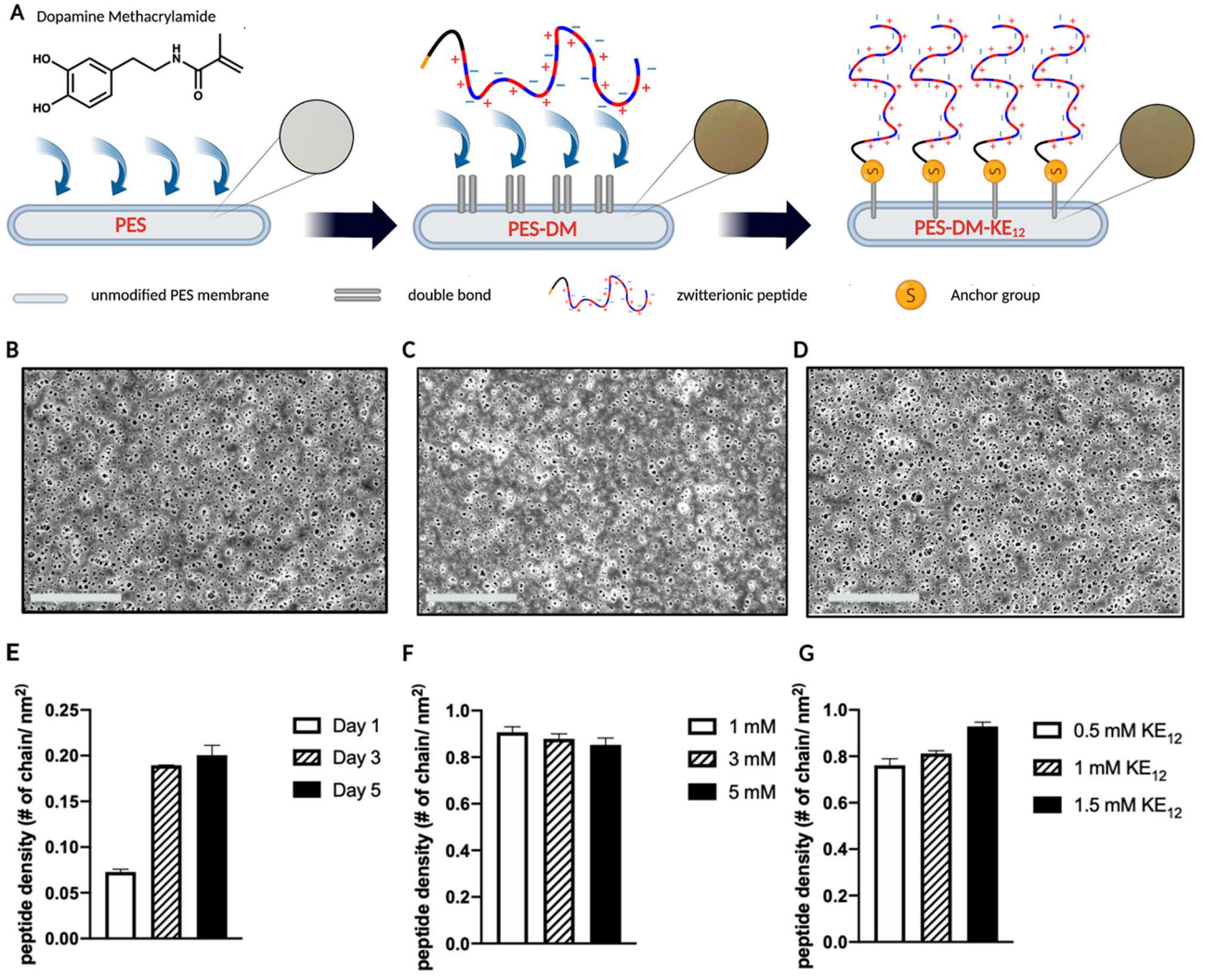

Figure 3. Illustration and characterization of PES membrane modification. (A) Schematic representation of the PES membrane modification steps, highlighting the intermediate PES-DM membrane used to attach zwitterionic peptides. The zoomed-in images show the membrane state at each modification stage. SEM images of (B) unmodified PES membrane with an average pore size of 431 ± 30.9 nm, (C) intermediate PES-DM membrane with an average pore size of 415 ± 20.8 nm, and (D) zwitterionic peptide-modified PES membrane (PES-DM-KE12) with an average pore size of 457 ± 21.1 nm. The scale bar represents 10 μm. Data are presented as mean ± SD, with n = 100 for each membrane. Peptide grafting density, represented as the number of peptide chains per nm,^{2} was analyzed by varying (E) incubation time, (F) DM concentration, and (G) KE12 concentration. Each error bar indicates the standard deviation of three independent measurements (n = 3).

charged residues. For the third peptide, we altered the linker design, replacing the four glycine residues with 11-mercaptoundecanoic acid, which consists of an 11-carbon hydrocarbon chain with a terminal thiol group and carboxylic acid. This linear hydrocarbon linker is more hydrophobic than the glycine-based linker. By varying the number of charged groups and linker designs, we could systematically evaluate their effects on antifouling performance. As a control molecule, we also designed and synthesized NZP, which contains 12 pairs of charged residues but lacks the zwitterionic characteristic. All amino acids used were selected as D-amino acids to reduce susceptibility to enzymatic degradation. The peptides were purified using HPLC, and their masses were confirmed via ESI (Figures S1−S4). Details of chemical synthesis and purification are included in the following Materials and Methods section.

The hypothesized antifouling mechanism of zwitterionic peptide-modified substrates is illustrated in Figure 1B. In the illustration, the zwitterionic peptides are shown attached to the substrate, with alternating positively charged (red segments) and negatively charged (blue segments) amino acid residues. These peptides are anchored to the substrate via an anchor group (orange) and a linker (black). The charged groups within the peptide chains attract and retain water molecules, forming a dense hydration shell (depicted as blue molecules). This hydration shell acts as a physical and energetic barrier, effectively preventing the adsorption of a wide range of foulants including proteins, cells, cell debris, enzymes, DNA/RNA, and organic molecules.

ZWITTERIONIC PEPTIDE-MODIFIED GOLD CHIPS AND NONSPECIFIC PROTEIN ADSORPTION

We first investigated the nonspecific protein adsorption of zwitterionic peptide-modified gold chips. The preparation of zwitterionic peptide-modified gold chips is detailed in the Materials and Methods section, and the nonspecific protein adsorption assay is illustrated in Figure 2A. In this study, zwitterionic peptides (1 mg/mL) were covalently attached to

https://doi.org/10.1021/acs.langmuir.4c04384
Langmuir 2025, 41, 1057−1067

gold chips using well-established thiol-gold chemistry.[46,52,53] This approach leverages the strong affinity between the thiol groups of cysteine residues and the gold substrate to ensure a stable peptide coating. The effectiveness of the zwitterionic peptides in resisting nonspecific protein adsorption was assessed using a sonication-based technique, which allows the quantification of loosely adsorbed proteins and foulants. The sonication process effectively removes noncovalently bound proteins from the gold surface, and the collected sonication solution was analyzed using UV−vis spectroscopy. By employing Beer's Law and the known absorptivity value of the IgG protein solution, we determined the mass of proteins adsorbed on the gold chips (Figure 2A).

A comparison between zwitterionic peptide-modified gold chips and plain gold chips (PGCs) clearly demonstrated the superior antifouling properties of the modified surfaces (Figure 2B). PGCs exhibited the highest level of protein adsorption at ∼13.3 ng/cm^2, indicating minimal antifouling resistance and serving as a baseline for comparison. Among the zwitterionic peptides tested, KE12 showed the most pronounced antifouling performance with a low adsorption level of approximately 2.2 ng/cm^2. MKE and KE8, by comparison, demonstrated adsorption levels of ∼4.2 and ∼7.4 ng/cm^2, respectively. Both KE12 and MKE fell below the commonly accepted ultralow fouling threshold of 5 ng/cm^2, indicating their ability to effectively resist protein adsorption through the formation of a zwitterionic hydration shell. The difference in the adsorption levels between KE12 and MKE may be attributed to variations in their linker designs. In contrast, the control molecule NZP, which lacks zwitterionic characteristics, exhibited higher protein adsorption at 9.5 ng/cm^2. These findings underscore the importance of optimizing both the zwitterionic characteristics and linker design as well as incorporating a higher number of lysine−glutamic acid pairs to enhance antifouling efficacy.

To further validate the antifouling capabilities of zwitterionic peptides under different conditions, we extended our analysis to cell culture media. Figure 2C,D presents the adsorption levels of various gold chips in fresh (Day 0) and aged (Day 7) cell culture media, respectively. Consistent with the results obtained using IgG protein solutions, KE12-modified gold chips showed the lowest adsorption levels, demonstrating robust antifouling properties, even in complex biological environments. To challenge the antifouling performance of the modified gold chips under extreme conditions, we exposed them to lysed cell solutions and measured the absorbance at three key wavelengths: 280, 260, and 220 nm (Figure 2E−G). Absorbance at 280 nm indicates the presence of most proteins, that at 260 nm indicates nucleic acids (DNA and RNA), and that at 220 nm corresponds to amino acids. Across all wavelengths, KE12 consistently exhibited the best antifouling performance among all tested peptides, indicating its broad-spectrum resistance to various foulants under the extreme lysed cell conditions.

PES Membrane Modification and Characterization. The protein-resisting performance of zwitterionic peptide-modified gold chips prompted us to explore their application in polymeric membranes, given their widespread use in protein purification, water treatment, and medical devices. For this study, we selected a commercially available PES membrane, commonly used in tangential flow filtration systems for protein purification. As illustrated in Figure 3A, DM was first deposited onto the PES membrane to introduce reactive double bonds for peptide attachment. The deposition was facilitated and stabilized by hydrogen bonding interactions, with the hydroxyl groups of DM's catechol moiety forming hydrogen bonds with the oxygen atoms in the ether linkages of the PES membrane. DM is a brownish powder that is soluble under slightly basic conditions, and successful deposition was visually confirmed by a color change of the membrane from white to orange. We utilized thiol−ene chemistry, a versatile organic reaction that forms a stable thioether bond between thiol groups and alkenes, to anchor the zwitterionic peptides to the membrane surface. This robust thioether linkage provides a stable and reliable peptide attachment. For these studies, we selected KE12 as the zwitterionic peptide due to its superior performance demonstrated in our experiments with gold chips. The successful attachment of zwitterionic peptides was confirmed by using Fourier transform infrared spectroscopy (FTIR). We compared the FTIR spectra of PES-DM and PES-DM-KE12 (Figure S5). The successful thiol-ene reaction was evidenced by the disappearance of the C−H alkene bending peak at 1000−875 cm^{-1} and the emergence of a new C−S bond peak at 730−580 cm^{-1}, confirming the covalent attachment of the zwitterionic peptides.

Next, to determine whether the chemical modifications affected the membrane structure and pore size, we analyzed the surface morphology of the unmodified PES membrane, the dopamine-methacrylamide-modified PES membrane (PES-DM), and the zwitterionic peptide-modified PES membrane (PES-DM-KE12) using scanning electron microscopy (SEM), as shown in Figure 3B−D. Pore size measurements were conducted on 100 randomly selected regions for each membrane type. The KE12-modified PES membrane exhibited an average pore size of 457 ± 21.1 nm, which was consistent with that of both the unmodified PES membrane and the intermediate PES-DM membrane. This result indicates that the modification process did not alter the pore size, thereby preserving the membrane's functional integrity.

We further evaluated the grafting density of the modified membrane by altering the incubation conditions as the grafting density of zwitterionic peptides on the PES membrane is crucial for antifouling performance. The stability of surface modification and optimal peptide density are crucial factors affecting long-term antifouling performance. A higher grafting density generally correlates with enhanced antifouling effects. Figure 3E presents the impact of varying the peptide incubation times (1, 3, and 5 days). The results showed a significant increase in grafting density from Day 1 (0.07 chains/nm^2) to Day 3 (0.18 chains/nm^2), with a minor increase from Day 3 to Day 5 (0.2 chains/nm^2). These findings indicate that incubation times beyond 2 days contribute minimally to further increasing the grafting density. This optimization seems to strike a balance between achieving sufficient surface coverage and preserving the peptides' conformational freedom, which is crucial for effective hydration shell formation and antifouling performance. The stability of the surface modification was further validated through protein adsorption tests conducted under diverse conditions, including exposure to cell culture media and lysed cell solutions. Remarkably, the modified membranes consistently maintained their antifouling properties, demonstrating their robustness and suitability in challenging biological environments. We then assessed protein adsorption for the membranes incubated for different durations using a 1 mg/mL IgG solution (Figure S6A,B). The results aligned with the

https://doi.org/10.1021/acs.langmuir.4c04384
Langmuir 2025, 41, 1057−1067

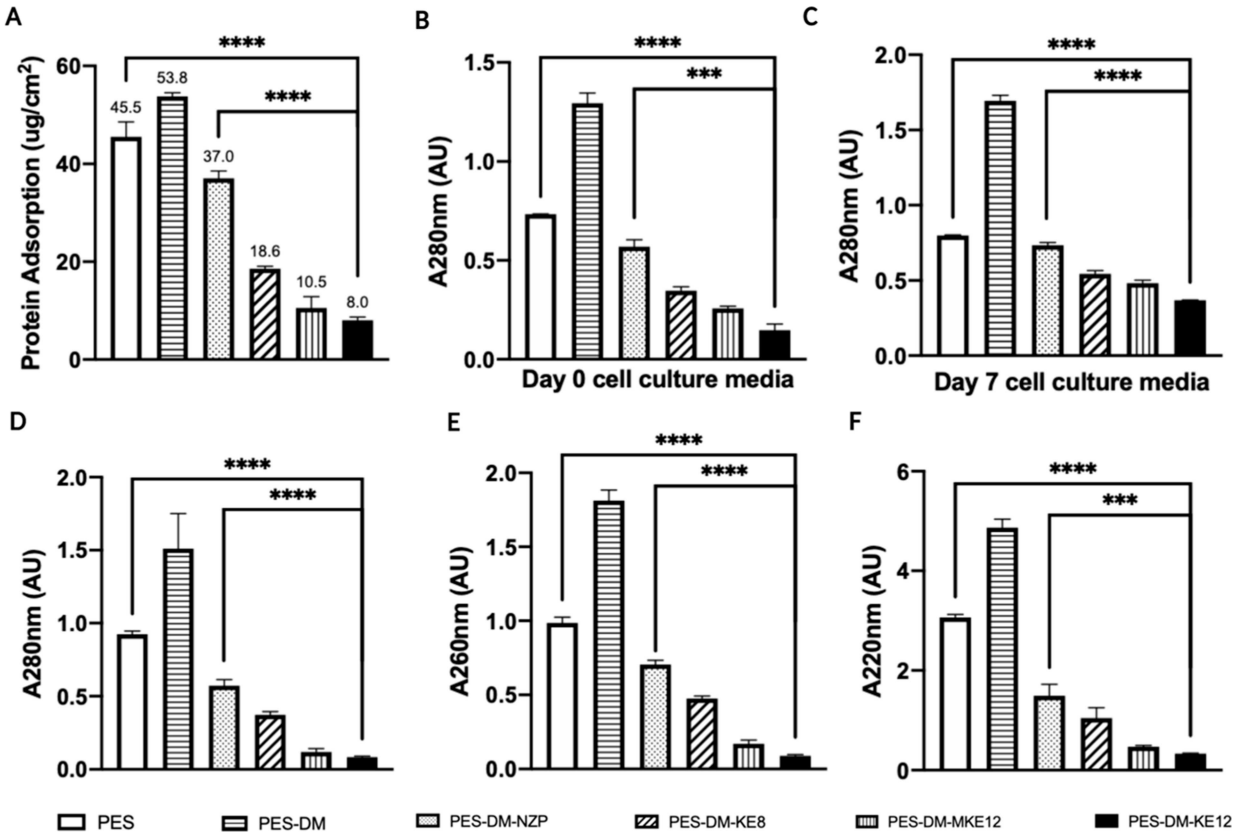

Figure 4. Antifouling performance of the modified PES membrane. (A) Antifouling performance of the unmodified PES membrane, intermediate PES membrane (PES-DM), nonzwitterionic control membrane (PES-DM-NZP) and zwitterionic peptide-modified membranes (PES-DM-KE8 and PES-DM-KE12) using a 1 mg/mL IgG protein solution, measured by UV−vis to determine protein adsorption per unit area. (B) Protein adsorption of the same membranes using fresh (Day 0) cell culture media, measured at 280 nm. (C) Protein adsorption of the same membranes using 7 day cell culture media, measured at 280 nm. (D−F) Adsorption of lysed cell culture media at (D) 280 nm, (E) 260 nm, and (F) 220 nm, measured for all membrane types. Each error bar represents the standard deviation of three independent measurements. Data are presented as mean ± SD (*$p < 0.05$; **$p < 0.01$; ns $p > 0.05$; and ****$p < 0.0001$ for KE12 vs unmodified PES and nonzwitterionic control membrane PES-DM-NZP; unpaired t-test, $n = 3$).

peptide density measurements, showing that higher peptide densities resulted in lower protein adsorption. Membranes incubated for 1 day adsorbed 1.3 μg/cm^2 of IgG, while those incubated for 3 and 5 days adsorbed approximately 0.9 μg/cm^2.

Another key factor affecting grafting density is the concentration of DM used in membrane modification. DM introduces double bonds onto the PES membrane while enabling zwitterionic peptide attachment via the thiol-ene chemistry. Interestingly, increasing the DM concentration from 1 to 3 and 5 mM did not significantly enhance peptide grafting density. Figure 3F compares DM concentrations of 1, 3, and 5 mM, showing a similar peptide density of approximately 0.9 chains/nm^2. However, protein adsorption increased as the DM concentration rose, especially from 1 to 3 mM, as illustrated in Figure S6C,D. Unexpectedly, higher DM concentrations resulted in increased protein adsorption, likely due to the adhesive nature of dopamine methacrylamide. Excess DM seems to enhance protein adherence to the membrane surface, thereby compromising its antifouling performance. Finally, we optimized the zwitterionic peptide concentration to achieve the highest grafting density, as shown in Figure 3G. A higher peptide concentration led to an increased grafting density and reduced protein adsorption, as confirmed by Figure S6E,F. Based on these findings, we determined the optimal conditions for the peptide grafting process to maximize antifouling performance in zwitterionic peptide-modified membranes.

Antifouling Performance of Modified PES Membranes in Static Conditions. We further evaluated the antifouling performance of zwitterionic peptide-modified PES membranes in various testing solutions, comparing them to unmodified PES membranes and intermediate PES-DM membranes. The same sonication technique was applied for this protein resistance assay, where lower protein adsorption indicated a better antifouling efficacy. The results mirrored the trends observed in the gold chip protein adsorption assay. As shown in Figure 4A, the unmodified PES membrane adsorbed 45.5 μg of IgG protein per cm^2, which is nearly six times higher than the adsorption observed for the KE12-modified membrane (8.0 μg/cm^2). Other zwitterionic peptide-modified membranes, such as PES-DM-KE8 and PES-DM-MKE, also demonstrated strong antifouling performance, though not as effectively as PES-DM-KE12.

Interestingly, the intermediate PES-DM membrane exhibited higher protein adsorption than the unmodified PES membrane, possibly due to the adhesive nature of dopamine methacrylamide, which may promote protein adherence. However, the zwitterionic peptide modification significantly improved the antifouling ability, resulting in lower protein

https://doi.org/10.1021/acs.langmuir.4c04384
Langmuir 2025, 41, 1057−1067

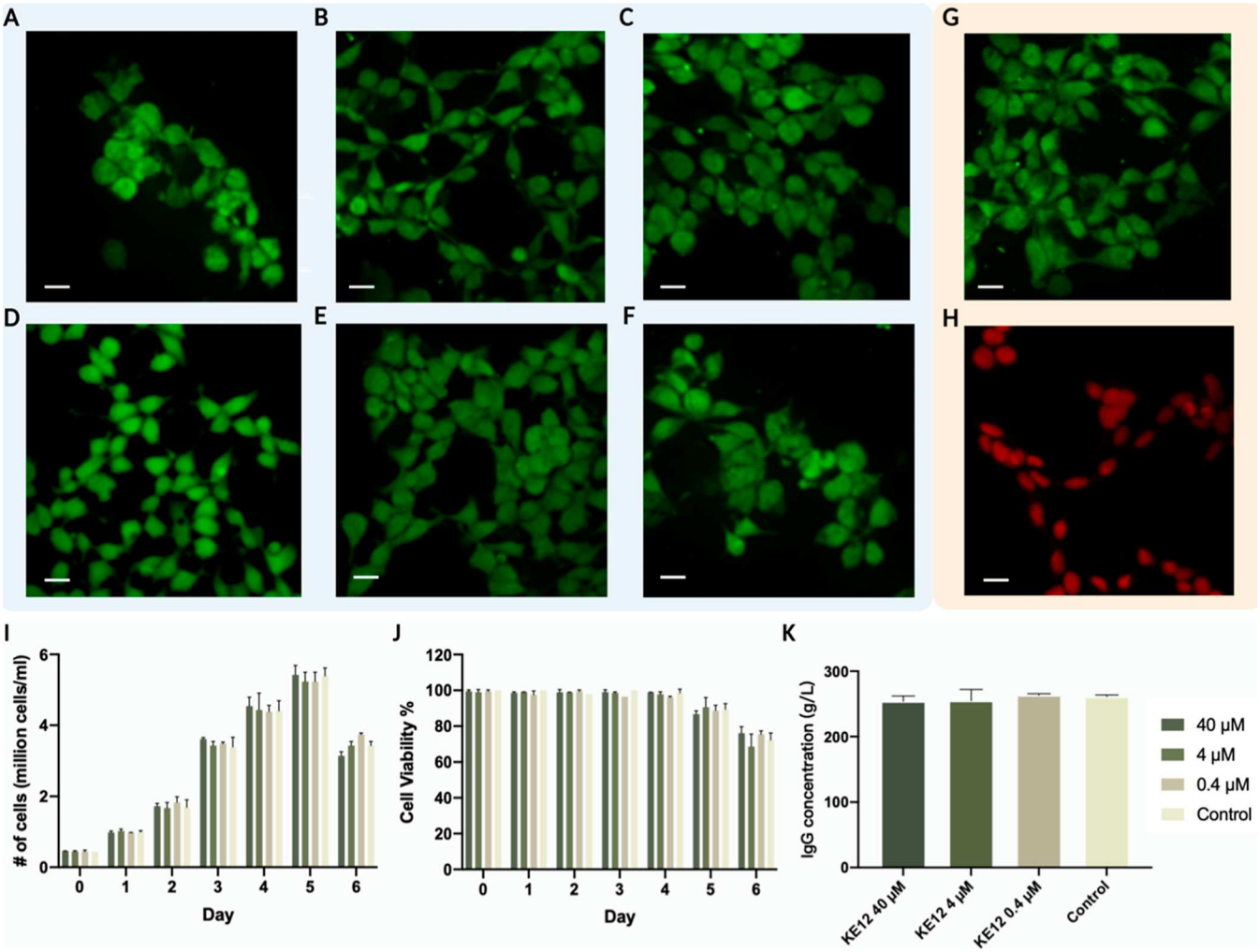

Figure 5. Cytotoxicity of KE12 peptides in the cell culture environment. Live/Dead cell viability confocal microscopy images of HEK 293 cells exposed to KE12 peptide solutions for 12 h at concentrations of (A) 0.4 μM, (B) 4 μM, and (C) 40 μM. Images of HEK 293 cells exposed to KE12 peptide solutions for 24 h at concentrations of (D) 0.4 μM, (E) 4 μM, and (F) 40 μM. (G) Positive control showing HEK 293 cells grown in media without zwitterionic peptides. (H) Negative control of HEK 293 cells treated with 70% ethanol. Images were acquired using a Zeiss LSM 780 confocal microscope with a 40× objective lens. Green fluorescence indicates live cells, and red fluorescence indicates dead/dying cells. Scale bars represent 50 μm. (I) Viable cell density, (J) cell viability, and (K) titer production of CHO cells cultivated in batch culture with 0.4, 4, and 40 μM KE12 peptide. For all conditions, the initial seeding day was designated as Day 0, and culture samples were collected every 24 h. Bars represent mean ± s.e.m.; $n = 3$. $^*p < 0.05$; NS, nonsignificant. Statistical analysis was performed using a two-tailed t-test compared to the control group.

adsorption levels compared to both unmodified and PES-DM membranes.

This trend was consistent across other testing solutions. Figure 4B,C demonstrates that zwitterionic peptide-modified membranes effectively resisted protein adsorption in a more complex cell culture environment. We measured the absorbance of the sonication solution at 280 nm for both fresh (Day 0) and aged (Day 7) cell culture media. Day 7 media contained a higher concentration of proteins, which explained the higher absorbance values across all membranes in Figure 4C compared to Figure 4B. In Figure 4D−F, we assessed membrane adsorption at 280, 260, and 220 nm, respectively, confirming consistent results with IgG protein solution and cell culture media. Interestingly, while KE12 consistently demonstrated the best antifouling performance, the magnitude of improvement over KE8 was not directly proportional to the 50% increase in the number of charged pairs. This observation can be attributed to two key factors. First, KE8, with its 8 pairs of charged groups, can already achieve strong antifouling properties through effective hydration layer formation. The additional charged pairs in KE12 enhance this hydration barrier, resulting in superior performance across all testing conditions, although the improvement is commensurate with the increase in charged KE pairs. Second, the longer chain length of KE12 may introduce greater steric hindrance, potentially reducing the surface grafting density of the peptides and limiting further gains in antifouling efficiency. Despite these considerations, KE12 consistently exhibited the best antifouling performance, indicating that the benefits of additional charged pairs outweigh any steric limitations introduced. These findings provide valuable insights into optimizing zwitterionic peptide design, emphasizing the importance of balancing charged group density with peptide chain length. The exceptional antifouling properties of KE12-modified membranes in both cell culture media and lysed cell environments highlight their potential for advanced protein purification applications.

https://doi.org/10.1021/acs.langmuir.4c04384
Langmuir 2025, 41, 1057−1067

Cytotoxicity of Zwitterionic Peptides in Cell Culture and Impact on Protein Production. We further assessed the cytotoxicity of the KE12 peptide in the HEK 293 cell line using confocal fluorescence microscopy, as shown in Figure 5A−H. Although our peptides are designed to remain covalently bound to substrates, we tested free peptides at concentrations far exceeding those that cells might encounter due to potential peptide detachment or degradation during protein production processes. This conservative approach ensures a rigorous and comprehensive safety evaluation of the biocompatibility of our system. The HEK 293 cell line, isolated from human kidney cells, is widely used for cell viability assays. Calcein AM and ethidium homodimer-1 were employed as fluorescence stains, where live cells fluoresced green and dead cells fluoresced red. We measured cell viability at two different time points (12 and 24 h) across three KE12 concentrations (0.4, 4, and 40 μM). The live control group was cultured in pure media without peptide addition, while the dead control group was treated with 70% ethanol. No dead cells were observed in the zwitterionic peptide-treated groups at either the 12 or 24 h time points, even at the highest concentration of 40 μM, which exceeds typical peptide concentrations in cell culture media that might result from potential surface detachment. These findings indicate that the zwitterionic peptides used in our study are nontoxic to the cell environment.

For a more comprehensive assessment, we conducted a batch process study on an IgG-expressing CHO cell line, exposing it to three different KE12 concentrations to examine the cytotoxicity. The results demonstrated that even at a concentration as high as 40 μM—significantly higher than any peptide concentrations resulting from detachment or degradation—there were no statistical differences in cell growth, viability, or titer production between the KE12-treated samples and the control samples throughout the batch process (Figure 5I−K). Protein A column HPLC was used for titer quantification measurement. To further validate these findings, we conducted a 14 day fed-batch experiment with the KE12 peptide, which displayed a similar trend and corroborated the results obtained from the initial batch process (Figure S7). It is worth noting that the observed decline in viable cell density and cell viability after Day 7 is typical for cells cultured under these conditions, with no significant differences detected between the KE12-treated samples and the control samples throughout the experiment. This consistency highlights that the presence of KE12 does not negatively impact cell growth or productivity, even over prolonged culture periods. Additionally, we assessed the impact of the MKE zwitterionic peptide and the dopamine methacrylamide intermediate on CHO cell growth to ensure that these components did not compromise cell viability. These investigations confirmed that neither the zwitterionic peptides nor the intermediate products had any adverse effects on CHO cell growth under the studied conditions. The corresponding data for these evaluations are provided in Figures S8 and S9. Overall, these results reinforce the biocompatibility of the zwitterionic peptides and intermediates, supporting their potential use in applications in which cell viability and sustained protein production are crucial.

CONCLUSIONS

In this study, we designed several zwitterionic peptides with varying numbers of charged groups and two different linker designs to investigate their antifouling performance. Our findings demonstrate that increasing the number of charged groups and enhancing hydrophilicity can significantly improve antifouling properties by promoting the formation of a more robust hydration shell. The successful attachment of zwitterionic peptides to both gold substrates and PES membranes highlights the versatility of our tunable peptide sequence design and modification chemistry. SEM imaging confirmed that the modification process did not alter the pore size or compromise the functionality of the PES membranes. Protein adsorption tests conducted across various environments—including protein solutions, cell culture media, and extreme lysed cell conditions—demonstrated the broad-spectrum antifouling effect of zwitterionic peptides. Furthermore, optimizing the zwitterionic peptide grafting density further enhanced the antifouling performance, indicating a clear pathway for improvement. The optimized grafting conditions identified in this study offer practical applications in protein purification and membrane separation industries, where they can help prolong the membrane lifespan and reduce operational costs. These insights into the key determinants of antifouling properties provide a valuable framework for designing more effective membrane modifications.

ASSOCIATED CONTENT

Supporting Information

The Supporting Information is available free of charge at https://pubs.acs.org/doi/10.1021/acs.langmuir.4c04384.

Characterization of synthesized peptide compounds (HPLC and ESI); FTIR characterization of the modified membranes; zwitterionic peptide grafting density corresponding to their antifouling performance; and effect of free zwitterionic peptides and the used dopamine on CHO cell growth in batch mode (PDF)

AUTHOR INFORMATION

Corresponding Author

Honggang Cui − *Department of Chemical and Biomolecular Engineering, Johns Hopkins University, Baltimore, Maryland 21218, United States; Institute for NanoBioTechnology and Department of Materials Science and Engineering, Johns Hopkins University, Baltimore, Maryland 21218, United States; Department of Oncology and Sidney Kimmel Comprehensive Cancer Center, Johns Hopkins University School of Medicine, Baltimore, Maryland 21205, United States;* orcid.org/0000-0002-4684-2655; Email: hcui6@jhu.edu

Authors

Boran Sun − *Department of Chemical and Biomolecular Engineering, Johns Hopkins University, Baltimore, Maryland 21218, United States; Institute for NanoBioTechnology, Johns Hopkins University, Baltimore, Maryland 21218, United States*

Junneng Wen − *Department of Chemical and Biomolecular Engineering, Johns Hopkins University, Baltimore, Maryland 21218, United States*

Meng Qin − *Department of Chemical and Biomolecular Engineering, Johns Hopkins University, Baltimore, Maryland 21218, United States; Institute for NanoBioTechnology,*

https://doi.org/10.1021/acs.langmuir.4c04384
Langmuir 2025, 41, 1057−1067

Johns Hopkins University, Baltimore, Maryland 21218, United States

Pranay Ladiwala − *Department of Chemical and Biomolecular Engineering, Johns Hopkins University, Baltimore, Maryland 21218, United States*

David Stern − *Department of Chemical and Biomolecular Engineering, Johns Hopkins University, Baltimore, Maryland 21218, United States; Institute for NanoBioTechnology, Johns Hopkins University, Baltimore, Maryland 21218, United States*

Ziying Xu − *Department of Chemical and Biomolecular Engineering, Johns Hopkins University, Baltimore, Maryland 21218, United States*

Michael J. Betenbaugh − *Department of Chemical and Biomolecular Engineering, Johns Hopkins University, Baltimore, Maryland 21218, United States;* orcid.org/0000-0002-1237-5550

Complete contact information is available at: https://pubs.acs.org/10.1021/acs.langmuir.4c04384

Notes

The authors declare no competing financial interest.

■ ACKNOWLEDGMENTS

This work was supported by the Advanced Mammalian Biomanufacturing Innovation Center (AMBIC, NSF 1624684). We also acknowledge the Johns Hopkins University Integrated Imaging Center for confocal microscopy imaging and the Department of Chemistry for mass spectrometry studies. We extend our gratitude to Dr. Christina Carbrello from Millipore Sigma for providing the unmodified PES membrane and to AMBIC industrial members for their valuable industry insights and suggestions.

■ REFERENCES

(1) Krishnan, S.; Weinman, C. J.; Ober, C. K. Advances in polymers for anti-biofouling surfaces. *J. Mater. Chem.* **2008**, *18* (29), 3405−3413.

(2) Banerjee, I.; Pangule, R. C.; Kane, R. S. Antifouling coatings: recent developments in the design of surfaces that prevent fouling by proteins, bacteria, and marine organisms. *Adv. Mater.* **2011**, *23* (6), 690−718.

(3) Zhang, P.; Sun, F.; Tsao, C.; Liu, S. J.; Jain, P.; Sinclair, A.; Hung, H. C.; Bai, T.; Wu, K.; Jiang, S. Y. Zwitterionic gel encapsulation promotes protein stability, enhances pharmacokinetics, and reduces immunogenicity. *Proc. Natl. Acad. Sci. U.S.A.* **2015**, *112* (39), 12046−12051.

(4) Flemming, H. C.; Schaule, G.; Griebe, T.; Schmitt, J.; Tamachkiarowa, A. Biofouling—the Achilles heel of membrane processes. *Desalination* **1997**, *113* (2−3), 215−225.

(5) Li, Q. S.; Wen, C. Y.; Yang, J.; Zhou, X. C.; Zhu, Y. N.; Zheng, J.; Cheng, G.; Bai, J.; Xu, T.; Ji, J.; et al. Zwitterionic Biomaterials. *Chem. Rev.* **2022**, *122* (23), 17073−17154.

(6) McMullen, P.; Luozhong, S.; Tsao, C.; Xu, H. X.; Fang, L.; Jiang, S. Y. A low-immunogenic genetically-fusible zwitterionic polypeptide. *Nano Today* **2022**, *47*, 101674.

(7) Wang, Z. J.; Delille, F.; Bartier, S.; Pons, T.; Lequeux, N.; Louis, B.; Kim, J.; Gacoin, T. Zwitterionic Polymers toward the Development of Orientation-Sensitive Bioprobes. *Langmuir* **2022**, *38* (34), 10512−10519.

(8) Jiang, S. Y.; Ishihara, K.; Iwasaki, Y.; Vancso, J. Zwitterionic Interfaces: Concepts and Emerging Applications Special Issue Preface. *Langmuir* **2019**, *35* (5), 1055.

(9) Vasilev, K.; Cook, J.; Griesser, H. J. Antibacterial surfaces for biomedical devices. *Expert Rev. Med. Devices* **2009**, *6* (5), 553−567.

(10) Werner, C.; Maitz, M. F.; Sperling, C. Current strategies towards hemocompatible coatings. *J. Mater. Chem.* **2007**, *17* (32), 3376−3384.

(11) Wisniewski, N.; Reichert, M. Methods for reducing biosensor membrane biofouling. *Colloids Surf., B* **2000**, *18* (3−4), 197−219.

(12) Guo, W.; Ngo, H. H.; Li, J. A mini-review on membrane fouling. *Bioresour. Technol.* **2012**, *122*, 27−34.

(13) Jiang, S. Y.; Cao, Z. Q. Ultralow-Fouling, Functionalizable, and Hydrolyzable Zwitterionic Materials and Their Derivatives for Biological Applications. *Adv. Mater.* **2010**, *22* (9), 920−932.

(14) Kwon, B.; Molek, J.; Zydney, A. L. Ultrafiltration of PEGylated proteins: Fouling and concentration polarization effects. *J. Membr. Sci.* **2008**, *319* (1−2), 206−213.

(15) Lowe, S.; O'Brien-Simpson, N. M.; Connal, L. A. Antibiofouling polymer interfaces: poly(ethylene glycol) and other promising candidates. *Polym. Chem.* **2015**, *6* (2), 198−212.

(16) Schlenoff, J. B. Z. Zwitteration: Coating Surfaces with Zwitterionic Functionality to Reduce Nonspecific Adsorption. *Langmuir* **2014**, *30* (32), 9625−9636.

(17) Cheng, G.; Zhang, Z.; Chen, S.; Bryers, J. D.; Jiang, S. Inhibition of bacterial adhesion and biofilm formation on zwitterionic surfaces. *Biomaterials* **2007**, *28* (29), 4192−4199.

(18) Zeng, Z.; Chen, S.; Chen, Y. Zwitterionic Polymer: A New Paradigm for Protein Conjugation beyond PEG. *ChemMedChem* **2023**, *18* (20), No. e202300245.

(19) Lin, C. H.; Luo, S. C. Zwitterionic Conducting Polymers: From Molecular Design, Surface Modification, and Interfacial Phenomenon to Biomedical Applications. *Langmuir* **2022**, *38* (24), 7383−7399.

(20) Willcox, M. D. P.; Hume, E. B. H.; Aliwarga, Y.; Kumar, N.; Cole, N. A novel cationic-peptide coating for the prevention of microbial colonization on contact lenses. *J. Appl. Microbiol.* **2008**, *105* (6), 1817−1825.

(21) Mi, L.; Jiang, S. Y. Integrated Antimicrobial and Nonfouling Zwitterionic Polymers. *Angew. Chem., Int. Ed.* **2014**, *53* (7), 1746−1754.

(22) Kim, I.; Kang, S. M. Formation of Amphiphilic Zwitterionic Thin Poly(SBMA-co-TFEMA) Brushes on Solid Surfaces for Marine Antifouling Applications. *Langmuir* **2024**, *40* (6), 3213−3221.

(23) Singh, N. K.; Wang, Y.; Wen, C.; Davis, B.; Wang, X.; Lee, K.; Wang, Y. High-affinity one-step aptamer selection using a non-fouling porous hydrogel. *Nat. Biotechnol.* **2024**, *42* (8), 1224−1231.

(24) Holmlin, R. E.; Chen, X. X.; Chapman, R. G.; Takayama, S.; Whitesides, G. M. Zwitterionic SAMs that resist nonspecific adsorption of protein from aqueous buffer. *Langmuir* **2001**, *17* (9), 2841−2850.

(25) Huang, H.; Zhang, C. C.; Crisci, R.; Lu, T. Y.; Hung, H. C.; Sajib, M. S. J.; Sarker, P.; Ma, J. R.; Wei, T.; Jiang, S. Y.; et al. Strong Surface Hydration and Salt Resistant Mechanism of a New Nonfouling Zwitterionic Polymer Based on Protein Stabilizer TMAO. *J. Am. Chem. Soc.* **2021**, *143* (40), 16786−16795.

(26) Imbia, A. S.; Ounkaew, A.; Mao, X. H.; Zeng, H. B.; Liu, Y.; Narain, R. Tannic Acid-Based Coatings Containing Zwitterionic Copolymers for Improved Antifouling and Antibacterial Properties. *Langmuir* **2024**, *40* (7), 3549−3558.

(27) Li, D.; Wei, Q.; Wu, C.; Zhang, X.; Xue, Q.; Zheng, T.; Cao, M. Superhydrophilicity and strong salt-affinity: Zwitterionic polymer grafted surfaces with significant potentials particularly in biological systems. *Adv. Colloid Interface Sci.* **2020**, *278*, 102141.

(28) Chen, Z. Surface Hydration and Antifouling Activity of Zwitterionic Polymers. *Langmuir* **2022**, *38* (16), 4483−4489.

(29) Del Grosso, C. A.; Leng, C.; Zhang, K. X.; Hung, H. C.; Jiang, S. Y.; Chen, Z.; Wilker, J. J. Surface hydration for antifouling and bioadhesion. *Chem. Sci.* **2020**, *11* (38), 10367−10377.

(30) Sarker, P.; Lu, T. Y.; Liu, D.; Wu, G. Y.; Chen, H. N.; Jahan Sajib, M. S.; Jiang, S. Y.; Chen, Z.; Wei, T. Hydration behaviors of nonfouling zwitterionic materials. *Chem. Sci.* **2023**, *14* (27), 7500−7511.

(31) Chen, S. H.; Chang, Y.; Lee, K. R.; Wei, T. C.; Higuchi, A.; Ho, F. M.; Tsou, C. C.; Ho, H. T.; Lai, J. Y. Hemocompatible control of

sulfobetaine-grafted polypropylene fibrous membranes in human whole blood via plasma-induced surface zwitterionization. *Langmuir* **2012**, *28* (51), 17733−17742.
(32) Chen, S.; Zheng, J.; Li, L.; Jiang, S. Strong Resistance of Phosphorylcholine Self-Assembled Monolayers to Protein Adsorption: Insights into Nonfouling Properties of Zwitterionic Materials. *J. Am. Chem. Soc.* **2005**, *127* (41), 14473−14478.
(33) Chen, S.; Liu, L.; Jiang, S. Strong Resistance of Oligo(phosphorylcholine) Self-Assembled Monolayers to Protein Adsorption. *Langmuir* **2006**, *22* (6), 2418−2421.
(34) Cheng, G.; Li, G. Z.; Xue, H.; Chen, S. F.; Bryers, J. D.; Jiang, S. Y. Zwitterionic carboxybetaine polymer surfaces and their resistance to long-term biofilm formation. *Biomaterials* **2009**, *30* (28), 5234−5240.
(35) Higaki, Y.; Furusawa, R.; Otsu, T.; Yamada, N. L. Zwitterionic Poly(carboxybetaine) Brush/Albumin Conjugate Films: Structure and Lubricity. *Langmuir* **2022**, *38* (30), 9278−9284.
(36) Kostina, N. Y.; Rodriguez-Emmenegger, C.; Houska, M.; Brynda, E.; Michálek, J. Non-fouling Hydrogels of 2-Hydroxyethyl Methacrylate and Zwitterionic Carboxybetaine (Meth)acrylamides. *Biomacromolecules* **2012**, *13* (12), 4164−4170.
(37) Naito, N.; Ukita, R.; Wilbs, J.; Wu, K.; Lin, X.; Carleton, N. M.; Roberts, K.; Jiang, S.; Heinis, C.; Cook, K. E. Combination of polycarboxybetaine coating and factor XII inhibitor reduces clot formation while preserving normal tissue coagulation during extracorporeal life support. *Biomaterials* **2021**, *272*, 120778.
(38) Zhang, Z.; Chao, T.; Chen, S. F.; Jiang, S. Y. Superlow fouling sulfobetaine and carboxybetaine polymers on glass slides. *Langmuir* **2006**, *22* (24), 10072−10077.
(39) Mondo, G. B.; Cathcarth, M.; Longo, G. S.; Picco, A. S.; Cardoso, M. B. Short Zwitterionic Sulfobetaine-Modified Silica Nanoparticles: Is Neutrality Possible? *Langmuir* **2024**, *40* (21), 10856−10867.
(40) Schönemann, E.; Koc, J.; Karthäuser, J. F.; Özcan, O.; Schanzenbach, D.; Schardt, L.; Rosenhahn, A.; Laschewsky, A. Sulfobetaine Methacrylate Polymers of Unconventional Polyzwitterion Architecture and Their Antifouling Properties. *Biomacromolecules* **2021**, *22* (4), 1494−1508.
(41) Wang, P. X.; Geiger, C.; Kreuzer, L. P.; Widmann, T.; Reitenbach, J.; Liang, S. Z.; Cubitt, R.; Henschel, C.; Laschewsky, A.; Papadakis, C. M.; et al. Poly(sulfobetaine)-Based Diblock Copolymer Thin Films in Water/Acetone Atmosphere: Modulation of Water Hydration and Co-nonsolvency-Triggered Film Contraction. *Langmuir* **2022**, *38* (22), 6934−6948.
(42) Overby, C.; Park, S.; Summers, A.; Benoit, D. S. W. Zwitterionic peptides: Tunable next-generation stealth nanoparticle modifications. *Bioactive Mater.* **2023**, *27*, 113−124.
(43) Qiao, X. J.; Qian, Z. H.; Sun, W. P.; Zhu, C. Y.; Li, Y. X.; Luo, X. L. Phosphorylation of Oligopeptides: Design of Ultra-Hydrophilic Zwitterionic Peptides for Anti-Fouling Detection of Nucleic Acids in Saliva. *Anal. Chem.* **2023**, *95* (29), 11091−11098.
(44) Cui, Z.; Wang, Y.; Zhang, L.; Qi, H. Zwitterionic Peptides: From Mechanism, Design Strategies to Applications. *ACS Appl. Mater. Interfaces* **2024**, *16* (42), 56497−56518.
(45) Chen, S. F.; Cao, Z. Q.; Jiang, S. Y. Ultra-low fouling peptide surfaces derived from natural amino acids. *Biomaterials* **2009**, *30* (29), 5892−5896.
(46) Ye, H.; Wang, L.; Huang, R.; Su, R.; Liu, B.; Qi, W.; He, Z. Superior Antifouling Performance of a Zwitterionic Peptide Compared to an Amphiphilic, Non-Ionic Peptide. *ACS Appl. Mater. Interfaces* **2015**, *7* (40), 22448−22457.
(47) Li, C. X.; Liu, C. J.; Li, M. L.; Xu, X.; Li, S. Z.; Qi, W.; Su, R. X.; Yu, J. Structures and Antifouling Properties of Self-Assembled Zwitterionic Peptide Monolayers: Effects of Peptide Charge Distributions and Divalent Cations. *Biomacromolecules* **2020**, *21* (6), 2087−2095.
(48) Kim, Y.; Binauld, S.; Stenzel, M. H. Zwitterionic Guanidine-Based Oligomers Mimicking Cell-Penetrating Peptides as a Nontoxic Alternative to Cationic Polymers to Enhance the Cellular Uptake of Micelles. *Biomacromolecules* **2012**, *13* (10), 3418−3426.
(49) Kozuka, Y.; Masuda, T.; Isu, N.; Takai, M. Antimicrobial Peptide Assembly on Zwitterionic Polymer Films to Slow Down Biofilm Formation. *Langmuir* **2024**, *40* (13), 7029−7037.
(50) Wang, Y.; Cheetham, A. G.; Angacian, G.; Su, H.; Xie, L.; Cui, H. Peptide−drug conjugates as effective prodrug strategies for targeted delivery. *Adv. Drug Deliv. Rev.* **2017**, *110*, 112−126.
(51) Cui, H.; Webber, M. J.; Stupp, S. I. Self-assembly of peptide amphiphiles: From molecules to nanostructures to biomaterials. *Pept. Sci.* **2010**, *94* (1), 1−18.
(52) Zheng, C. B.; Alvisi, N.; de Haas, R. J.; Zhang, Z. S.; Zuilhof, H.; de Vries, R. Modular Design for Proteins Assembling into Antifouling Coatings: Case of Gold Surfaces. *Langmuir* **2023**, *39* (27), 9290−9299.
(53) Liu, Q. S.; Singh, A.; Lalani, R.; Liu, L. Y. Ultralow Fouling Polyacrylamide on Gold Surfaces via Surface-Initiated Atom Transfer Radical Polymerization. *Biomacromolecules* **2012**, *13* (4), 1086−1092.

https://doi.org/10.1021/acs.langmuir.4c04384
Langmuir 2025, 41, 1057−1067